

MIT Open Access Articles

Search for mixing-induced CP violation using partial reconstruction of $[\bar{B}]^0 \rightarrow D^{+} X^0[\bar{v}]_{\#}$ and kaon tagging*

The MIT Faculty has made this article openly available. **Please share** how this access benefits you. Your story matters.

Citation: Lees, J. P., V. Poireau, V. Tisserand, E. Grauges, et al. "Search for mixing-induced CP violation using partial reconstruction of $[\bar{B}]^0 \rightarrow D^{*+} X^0[\bar{v}]_{\#}$ and kaon tagging." Phys. Rev. D 93, 032001 (February 2016). © 2016 American Physical Society

As Published: <http://dx.doi.org/10.1103/PhysRevD.93.032001>

Publisher: American Physical Society

Persistent URL: <http://hdl.handle.net/1721.1/101137>

Version: Final published version: final published article, as it appeared in a journal, conference proceedings, or other formally published context

Terms of Use: Article is made available in accordance with the publisher's policy and may be subject to US copyright law. Please refer to the publisher's site for terms of use.



Search for mixing-induced CP violation using partial reconstruction of $\bar{B}^0 \rightarrow D^{*+} X \ell^- \bar{\nu}_\ell$ and kaon tagging

J. P. Lees,¹ V. Poireau,¹ V. Tisserand,¹ E. Grauges,² A. Palano,^{3a,3b} G. Eigen,⁴ B. Stugu,⁴ D. N. Brown,⁵ L. T. Kerth,⁵
 Yu. G. Kolomensky,⁵ M. J. Lee,⁵ G. Lynch,⁵ H. Koch,⁶ T. Schroeder,⁶ C. Hearty,⁷ T. S. Mattison,⁷ J. A. McKenna,⁷
 R. Y. So,⁷ A. Khan,⁸ V. E. Blinov,^{9a,9b,9c} A. R. Buzykaev,^{9a} V. P. Druzhinin,^{9a,9b} V. B. Golubev,^{9a,9b} E. A. Kravchenko,^{9a,9b}
 A. P. Onuchin,^{9a,9b,9c} S. I. Serednyakov,^{9a,9b} Yu. I. Skovpen,^{9a,9b} E. P. Solodov,^{9a,9b} K. Yu. Todyshev,^{9a,9b}
 A. J. Lankford,¹⁰ B. Dey,¹¹ J. W. Gary,¹¹ O. Long,¹¹ M. Franco Sevilla,¹² T. M. Hong,¹² D. Kovalskyi,¹²
 J. D. Richman,¹² C. A. West,¹² A. M. Eisner,¹³ W. S. Lockman,¹³ W. Panduro Vazquez,¹³ B. A. Schumm,¹³ A. Seiden,¹³
 D. S. Chao,¹⁴ C. H. Cheng,¹⁴ B. Echenard,¹⁴ K. T. Flood,¹⁴ D. G. Hitlin,¹⁴ J. Kim,¹⁴ T. S. Miyashita,¹⁴
 P. Ongmongkolkul,¹⁴ F. C. Porter,¹⁴ M. Röhrken,¹⁴ R. Andreassen,¹⁵ Z. Huard,¹⁵ B. T. Meadows,¹⁵ B. G. Pushpawela,¹⁵
 M. D. Sokoloff,¹⁵ L. Sun,¹⁵ W. T. Ford,¹⁶ A. Gaz,¹⁶ J. G. Smith,¹⁶ S. R. Wagner,¹⁶ R. Ayad,^{17,†} W. H. Toki,¹⁷
 B. Spaan,¹⁸ D. Bernard,¹⁹ M. Verderi,¹⁹ S. Playfer,²⁰ D. Bettoni,^{21a} C. Bozzi,^{21a} R. Calabrese,^{21a,21b} G. Cibinetto,^{21a,21b}
 E. Fioravanti,^{21a,21b} I. Garzia,^{21a,21b} E. Luppi,^{21a,21b} L. Piemontese,^{21a} V. Santoro,^{21a} A. Calcaterra,²² R. de Sangro,²²
 G. Finocchiaro,²² S. Martellotti,²² P. Patteri,²² I. M. Peruzzi,²² M. Piccolo,²² A. Zallo,²² R. Contri,²² M. R. Monge,²²
 S. Passaggio,^{23a,23b} C. Patrignani,^{23a,23b} E. Robutti,^{23a} B. Bhuyan,²⁴ V. Prasad,²⁴ A. Adametz,²⁵ U. Uwer,²⁵
 H. M. Lacker,²⁶ U. Mallik,²⁷ C. Chen,²⁸ J. Cochran,²⁸ S. Prell,²⁸ H. Ahmed,²⁹ A. V. Gritsan,³⁰ N. Arnaud,³¹ M. Davier,³¹
 D. Derkach,³¹ G. Grosdidier,³¹ F. Le Diberder,³¹ A. M. Lutz,³¹ B. Malaescu,^{31,‡} P. Roudeau,³¹ A. Stocchi,³¹
 G. Wormser,³¹ D. J. Lange,³² D. M. Wright,³² J. P. Coleman,³³ J. R. Fry,³³ E. Gabathuler,³³ D. E. Hutchcroft,³³
 D. J. Payne,³³ C. Touramanis,³³ A. J. Bevan,³⁴ F. Di Lodovico,³⁴ R. Sacco,³⁴ G. Cowan,³⁵ D. N. Brown,³⁶ C. L. Davis,³⁶
 A. G. Denig,³⁷ M. Fritsch,³⁷ W. Gradl,³⁷ K. Griessinger,³⁷ A. Hafner,³⁷ K. R. Schubert,³⁷ R. J. Barlow,^{38,§}
 G. D. Lafferty,³⁸ R. Cenci,³⁹ B. Hamilton,³⁹ A. Jawahery,³⁹ D. A. Roberts,³⁹ R. Cowan,⁴⁰ R. Cheaib,⁴¹ P. M. Patel,^{41,*}
 S. H. Robertson,⁴¹ N. Neri,^{42a} F. Palombo,^{42a,42b} L. Cremaldi,^{43,||} R. Godang,^{43,||} D. J. Summers,⁴³ M. Simard,⁴⁴ P. Taras,⁴⁴
 G. De Nardo,^{45a,45b} G. Onorato,^{45a,45b} C. Sciacca,^{45a,45b} G. Raven,⁴⁶ C. P. Jessop,⁴⁷ J. M. LoSecco,⁴⁷ K. Honscheid,⁴⁸
 R. Kass,⁴⁸ M. Margoni,^{49a,49b} M. Morandin,^{49a} M. Posocco,^{49a} M. Rotondo,^{49a} G. Simi,^{49a,49b} F. Simonetto,^{49a,49b}
 R. Stroili,^{49a,49b} S. Akar,⁵⁰ E. Ben-Haim,⁵⁰ M. Bomben,⁵⁰ G. R. Bonneaud,⁵⁰ H. Briand,⁵⁰ G. Calderini,⁵⁰ J. Chauveau,⁵⁰
 Ph. Leruste,⁵⁰ G. Marchiori,⁵⁰ J. Ocariz,⁵⁰ M. Biasini,^{51a,51b} E. Manoni,^{51a} A. Rossi,^{51a} C. Angelini,^{52a,52b}
 G. Batignani,^{52a,52b} S. Bettarini,^{52a,52b} M. Carpinelli,^{52a,52b} G. Casarosa,^{52a,52b} M. Chrzascz,^{52a,52b} F. Forti,^{52a,52b}
 M. A. Giorgi,^{52a,52b} A. Lusiani,^{52a,52b} B. Oberhof,^{52a,52b} E. Paoloni,^{52a,52b} M. Rama,^{52a} G. Rizzo,^{52a,52b} J. J. Walsh,^{52a}
 D. Lopes Pegna,⁵³ J. Olsen,⁵³ A. J. S. Smith,⁵³ F. Anulli,^{54a} R. Faccini,^{54a} F. Ferrarotto,^{54a} F. Ferroni,^{54a,54b}
 M. Gaspero,^{54a,54b} A. Pilloni,^{54a,54b} G. Piredda,^{54a} C. Büniger,^{54a} S. Dittrich,⁵⁵ O. Grünberg,⁵⁵ M. Hess,⁵⁵ T. Leddig,⁵⁵
 C. Voß,⁵⁵ R. Waldi,⁵⁵ T. Adye,⁵⁶ E. O. Olaiya,⁵⁶ F. F. Wilson,⁵⁶ S. Emery,⁵⁷ G. Vasseur,⁵⁷ D. Aston,⁵⁸ D. J. Bard,⁵⁸
 C. Cartaro,⁵⁸ M. R. Convery,⁵⁸ J. Dorfan,⁵⁸ G. P. Dubois-Felsmann,⁵⁸ W. Dunwoodie,⁵⁸ M. Ebert,⁵⁸ R. C. Field,⁵⁸
 B. G. Fulsom,⁵⁸ M. T. Graham,⁵⁸ C. Hast,⁵⁸ W. R. Innes,⁵⁸ P. Kim,⁵⁸ D. W. G. S. Leith,⁵⁸ S. Luitz,⁵⁸ V. Luth,⁵⁸
 D. B. MacFarlane,⁵⁸ D. R. Muller,⁵⁸ H. Neal,⁵⁸ T. Pulliam,⁵⁸ B. N. Ratcliff,⁵⁸ A. Roodman,⁵⁸ R. H. Schindler,⁵⁸
 A. Snyder,⁵⁸ D. Su,⁵⁸ M. K. Sullivan,⁵⁸ J. Va'vra,⁵⁸ W. J. Wisniewski,⁵⁸ H. W. Wulsin,⁵⁸ M. V. Purohit,⁵⁹ J. R. Wilson,⁵⁹
 A. Randle-Conde,⁶⁰ S. J. Sekula,⁶⁰ M. Bellis,⁶¹ P. R. Burchat,⁶¹ E. M. T. Puccio,⁶¹ M. S. Alam,⁶² J. A. Ernst,⁶²
 R. Gorodeisky,⁶³ N. Guttman,⁶³ D. R. Peimer,⁶³ A. Soffer,⁶³ S. M. Spanier,⁶⁴ J. L. Ritchie,⁶⁵ R. F. Schwitters,⁶⁵
 J. M. Izen,⁶⁶ X. C. Lou,⁶⁶ F. Bianchi,^{67a,67b} F. De Mori,^{67a,67b} A. Filippi,^{67a} D. Gamba,^{67a,67b} L. Lanceri,^{68a,68b} L. Vitale,^{68a,68b}
 F. Martinez-Vidal,⁶⁹ A. Oyanguren,⁶⁹ J. Albert,⁷⁰ Sw. Banerjee,⁷⁰ A. Beaulieu,⁷⁰ F. U. Bernlochner,⁷⁰
 H. H. F. Choi,⁷⁰ G. J. King,⁷⁰ R. Kowalewski,⁷⁰ M. J. Lewczuk,⁷⁰ T. Lueck,⁷⁰ I. M. Nugent,⁷⁰ J. M. Roney,⁷⁰
 R. J. Sobie,⁷⁰ N. Tasneem,⁷⁰ T. J. Gershon,⁷¹ P. F. Harrison,⁷¹ T. E. Latham,⁷¹ H. R. Band,⁷² S. Dasu,⁷² Y. Pan,⁷²
 R. Prepost,⁷² and S. L. Wu⁷²
 (The BABAR Collaboration)

¹Laboratoire d'Annecy-le-Vieux de Physique des Particules (LAPP), Université de Savoie, CNRS/IN2P3, F-74941 Annecy-Le-Vieux, France

²Universitat de Barcelona, Facultat de Física, Departament ECM, E-08028 Barcelona, Spain

^{3a}INFN Sezione di Bari, I-70126 Bari, Italy

^{3b}Dipartimento di Fisica, Università di Bari, I-70126 Bari, Italy

⁴University of Bergen, Institute of Physics, N-5007 Bergen, Norway

⁵Lawrence Berkeley National Laboratory and University of California, Berkeley, California 94720, USA

⁶Ruhr Universität Bochum, Institut für Experimentalphysik 1, D-44780 Bochum, Germany

⁷University of British Columbia, Vancouver, British Columbia, Canada V6T 1Z1

⁸Brunel University, Uxbridge, Middlesex UB8 3PH, United Kingdom

- ^{9a}*Budker Institute of Nuclear Physics SB RAS, Novosibirsk 630090, Russia*
^{9b}*Russia Novosibirsk State University, Novosibirsk 630090, Russia*
^{9c}*Russia Novosibirsk State Technical University, Novosibirsk 630092, Russia*
¹⁰*University of California at Irvine, Irvine, California 92697, USA*
¹¹*University of California at Riverside, Riverside, California 92521, USA*
¹²*University of California at Santa Barbara, Santa Barbara, California 93106, USA*
¹³*University of California at Santa Cruz, Institute for Particle Physics, Santa Cruz, California 95064, USA*
¹⁴*California Institute of Technology, Pasadena, California 91125, USA*
¹⁵*University of Cincinnati, Cincinnati, Ohio 45221, USA*
¹⁶*University of Colorado, Boulder, Colorado 80309, USA*
¹⁷*Colorado State University, Fort Collins, Colorado 80523, USA*
¹⁸*Technische Universität Dortmund, Fakultät Physik, D-44221 Dortmund, Germany*
¹⁹*Laboratoire Leprince-Ringuet, Ecole Polytechnique, CNRS/IN2P3, F-91128 Palaiseau, France*
²⁰*University of Edinburgh, Edinburgh EH9 3JZ, United Kingdom*
^{21a}*INFN Sezione di Ferrara, I-44122 Ferrara, Italy*
^{21b}*Dipartimento di Fisica e Scienze della Terra, Università di Ferrara, I-44122 Ferrara, Italy*
²²*INFN Laboratori Nazionali di Frascati, I-00044 Frascati, Italy*
^{23a}*INFN Sezione di Genova, I-16146 Genova, Italy*
^{23b}*Dipartimento di Fisica, Università di Genova, I-16146 Genova, Italy*
²⁴*Indian Institute of Technology Guwahati, Guwahati, Assam, 781 039, India*
²⁵*Universität Heidelberg, Physikalisches Institut, D-69120 Heidelberg, Germany*
²⁶*Humboldt-Universität zu Berlin, Institut für Physik, D-12489 Berlin, Germany*
²⁷*University of Iowa, Iowa City, Iowa 52242, USA*
²⁸*Iowa State University, Ames, Iowa 50011-3160, USA*
²⁹*Physics Department, Jazan University, Jazan 22822, Kingdom of Saudi Arabia*
³⁰*Johns Hopkins University, Baltimore, Maryland 21218, USA*
³¹*Laboratoire de l'Accélérateur Linéaire, IN2P3/CNRS et Université Paris-Sud 11, Centre Scientifique d'Orsay, F-91898 Orsay Cedex, France*
³²*Lawrence Livermore National Laboratory, Livermore, California 94550, USA*
³³*University of Liverpool, Liverpool L69 7ZE, United Kingdom*
³⁴*Queen Mary, University of London, London E1 4NS, United Kingdom*
³⁵*University of London, Royal Holloway and Bedford New College, Egham, Surrey TW20 0EX, United Kingdom*
³⁶*University of Louisville, Louisville, Kentucky 40292, USA*
³⁷*Johannes Gutenberg-Universität Mainz, Institut für Kernphysik, D-55099 Mainz, Germany*
³⁸*University of Manchester, Manchester M13 9PL, United Kingdom*
³⁹*University of Maryland, College Park, Maryland 20742, USA*
⁴⁰*Massachusetts Institute of Technology, Laboratory for Nuclear Science, Cambridge, Massachusetts 02139, USA*
⁴¹*McGill University, Montréal, Québec, Canada H3A 2T8*
^{42a}*INFN Sezione di Milano, I-20133 Milano, Italy*
^{42b}*Dipartimento di Fisica, Università di Milano, I-20133 Milano, Italy*
⁴³*University of Mississippi, University, Mississippi 38677, USA*
⁴⁴*Université de Montréal, Physique des Particules, Montréal, Québec, Canada H3C 3J7*
^{45a}*INFN Sezione di Napoli, I-80126 Napoli, Italy*
^{45b}*Dipartimento di Scienze Fisiche, Università di Napoli Federico II, I-80126 Napoli, Italy*
⁴⁶*NIKHEF, National Institute for Nuclear Physics and High Energy Physics, NL-1009 DB Amsterdam, The Netherlands*
⁴⁷*University of Notre Dame, Notre Dame, Indiana 46556, USA*
⁴⁸*Ohio State University, Columbus, Ohio 43210, USA*
^{49a}*INFN Sezione di Padova, I-35131 Padova, Italy*
^{49b}*Dipartimento di Fisica, Università di Padova, I-35131 Padova, Italy*
⁵⁰*Laboratoire de Physique Nucléaire et de Hautes Energies, IN2P3/CNRS, Université Pierre et Marie Curie-Paris6, Université Denis Diderot-Paris7, F-75252 Paris, France*
^{51a}*INFN Sezione di Perugia, I-06123 Perugia, Italy*
^{51b}*Dipartimento di Fisica, Università di Perugia, I-06123 Perugia, Italy*
^{52a}*INFN Sezione di Pisa, I-56127 Pisa, Italy*
^{52b}*Dipartimento di Fisica, Università di Pisa, I-56127 Pisa, Italy*
^{52c}*Scuola Normale Superiore di Pisa, I-56127 Pisa, Italy*
⁵³*Princeton University, Princeton, New Jersey 08544, USA*

^{54a}INFN Sezione di Roma, I-00185 Roma, Italy^{54b}Dipartimento di Fisica, Università di Roma La Sapienza, I-00185 Roma, Italy⁵⁵Universität Rostock, D-18051 Rostock, Germany⁵⁶Rutherford Appleton Laboratory, Chilton, Didcot, Oxfordshire, OX11 0QX, United Kingdom⁵⁷CEA, Irfu, SPP, Centre de Saclay, F-91191 Gif-sur-Yvette, France⁵⁸SLAC National Accelerator Laboratory, Stanford, California 94309 USA⁵⁹University of South Carolina, Columbia, South Carolina 29208, USA⁶⁰Southern Methodist University, Dallas, Texas 75275, USA⁶¹Stanford University, Stanford, California 94305-4060, USA⁶²State University of New York, Albany, New York 12222, USA⁶³Tel Aviv University, School of Physics and Astronomy, Tel Aviv 69978, Israel⁶⁴University of Tennessee, Knoxville, Tennessee 37996, USA⁶⁵University of Texas at Austin, Austin, Texas 78712, USA⁶⁶University of Texas at Dallas, Richardson, Texas 75083, USA^{67a}INFN Sezione di Torino, I-10125 Torino, Italy^{67b}Dipartimento di Fisica, Università di Torino, I-10125 Torino, Italy^{68a}INFN Sezione di Trieste, I-34127 Trieste, Italy^{68b}Dipartimento di Fisica, Università di Trieste, I-34127 Trieste, Italy⁶⁹IFIC, Universitat de Valencia-CSIC, E-46071 Valencia, Spain⁷⁰University of Victoria, Victoria, British Columbia, Canada V8W 3P6⁷¹Department of Physics, University of Warwick, Coventry CV4 7AL, United Kingdom⁷²University of Wisconsin, Madison, Wisconsin 53706, USA

(Received 8 June 2015; revised manuscript received 23 December 2015; published 8 February 2016)

We describe in detail a previously published measurement of CP violation in B^0 - \bar{B}^0 oscillations, based on an integrated luminosity of 425.7 fb^{-1} collected by the BABAR experiment at the PEP-II collider. We apply a novel technique to a sample of about 6 million $\bar{B}^0 \rightarrow D^{*+} \ell^- \bar{\nu}_\ell$ decays selected with partial reconstruction of the D^{*+} meson. The charged lepton identifies the flavor of one B meson at its decay time, the flavor of the other B is determined by kaon tagging. We determine a CP violating asymmetry $\mathcal{A}_{CP} = (N(B^0 \bar{B}^0) - N(\bar{B}^0 B^0)) / (N(B^0 \bar{B}^0) + N(\bar{B}^0 B^0)) = (0.06 \pm 0.17^{+0.38}_{-0.32})\%$ corresponding to $\Delta_{CP} = 1 - |q/p| = (0.29 \pm 0.84^{+1.88}_{-1.61}) \times 10^{-3}$. This measurement is consistent and competitive with those obtained at the B factories with dilepton events.

DOI: 10.1103/PhysRevD.93.032001

I. INTRODUCTION

The time evolution of neutral B mesons is governed by the Schrödinger equation:

$$-i \frac{\partial}{\partial t} \Psi = \mathcal{H} \Psi \quad (1)$$

where $\Psi = \psi_1 |B^0\rangle + \psi_2 |\bar{B}^0\rangle$ and $B^0 = (\bar{b}d)$ and $\bar{B}^0 = (b\bar{d})$ are flavor eigenstates. Hamiltonian $\mathcal{H} = M - \frac{i}{2}\Gamma$ is the combination of two 2×2 Hermitian matrices, $M^\dagger = M$, $\Gamma^\dagger = \Gamma$ expressing dispersive and absorptive

contributions respectively. The two eigenstates of \mathcal{H} , with well-defined values of mass (m_L , m_H) and decay width (Γ_L , Γ_H), are expressed in terms of B^0 and \bar{B}^0 , as

$$\begin{aligned} |B_L\rangle &= p|B^0\rangle + q|\bar{B}^0\rangle \\ |B_H\rangle &= p|B^0\rangle - q|\bar{B}^0\rangle, \end{aligned} \quad (2)$$

where

$$\frac{q}{p} = \sqrt{\frac{M_{12}^* - i\Gamma_{12}^*/2}{M_{12} - i\Gamma_{12}/2}}. \quad (3)$$

The process of B^0 - \bar{B}^0 flavor mixing is therefore governed by two real parameters, $|M_{12}|$, $|\Gamma_{12}|$ and by the phase $\phi_{12} = \arg(-\Gamma_{12}/M_{12})$.

The value of $|M_{12}|$ is related to the frequency of B^0 - \bar{B}^0 oscillations, Δm , by the relation

$$\Delta m = m_H - m_L = 2|M_{12}|, \quad (4)$$

*Deceased.

[†]Present address: University of Tabuk, Tabuk 71491, Saudi Arabia.

[‡]Present address: Laboratoire de Physique Nucléaire et de Hautes Energies, IN2P3/CNRS, F-75252 Paris, France.

[§]Present address: University of Huddersfield, Huddersfield HD1 3DH, United Kingdom.

^{||}Present address: University of South Alabama, Mobile, Alabama 36688, USA.

[¶]Also at Università di Sassari, I-07100 Sassari, Italy.

whereas the following expression relates the decay width difference $\Delta\Gamma$ to $|\Gamma_{12}|$ and ϕ_{12} :

$$\Delta\Gamma = \Gamma_L - \Gamma_H = 2|\Gamma_{12}| \cos \phi_{12}. \quad (5)$$

A third observable probing mixing is the CP mixing asymmetry

$$\mathcal{A}_{CP} = \frac{\bar{\mathcal{P}} - \mathcal{P}}{\bar{\mathcal{P}} + \mathcal{P}} \simeq 2 \left(1 - \left| \frac{q}{p} \right| \right) = \frac{\Delta\Gamma}{\Delta m} \tan \phi_{12}, \quad (6)$$

where $\mathcal{P} = \text{prob}(B^0 \rightarrow \bar{B}^0)$ is the probability that a state, produced as a B^0 , decays as a \bar{B}^0 ; $\bar{\mathcal{P}} = \text{prob}(\bar{B}^0 \rightarrow B^0)$ is the probability for the CP conjugate oscillation; the second equality holds if $|q/p| \simeq 1$; and the last if $|\Gamma_{12}/M_{12}| \ll 1$.

In the Standard Model the dispersive term M_{12} is dominated by box diagrams involving two top quarks. Owing to the large top mass, a sizable value of Δm is expected. The measured value $\Delta m = 0.510 \pm 0.004 \text{ ps}^{-1}$ [1] is consistent with the SM expectation. The period corresponds to about eight times the B^0 average lifetime.

As only the few final states common to B^0 and \bar{B}^0 contribute to $|\Gamma_{12}|$, small values of $\Delta\Gamma$ and \mathcal{A}_{CP} are expected. One of the most recent theoretical calculations based on the SM [2], including NLO QCD correction, predicts

$$\Delta_{CP} = 1 - |q/p| \simeq \frac{1}{2} \mathcal{A}_{CP} = -(2.4_{-0.6}^{+0.5}) \times 10^{-4}. \quad (7)$$

Sizable deviations from zero would therefore be a clear indication of new physics (NP). A detailed review of possible NP contributions to CP violation in B^0 - \bar{B}^0 mixing can be found in [3]. In this paper, we describe the measurement of \mathcal{A}_{CP} performed by the BABAR Collaboration with a novel technique, previously published in [4], which, due to the analysis complexity, requires a more detailed description.

This article is organized as follows. An overview of the current experimental situation and the strategy of this measurement are reported in Sec. II. The BABAR detector is described briefly in Sec. III. Event selection and sample composition are then described in Sec. IV. Tagging the flavor of the B meson is described in Sec. V. The measurement of \mathcal{A}_{CP} is described in Sec. VI, the fit validation is described in Sec. VII, and the discussion of the systematic uncertainties follows in Sec. VIII, while we summarize the results and draw our conclusions in Secs. IX and X.

II. EXPERIMENTAL OVERVIEW AND DESCRIPTION OF THE MEASUREMENT

In hadron collider experiments, $b\bar{b}$ pairs produced at the parton level hadronize generating the b hadrons, which eventually decay weakly. In B factories, pairs of opposite

flavor B -mesons are produced through the process $e^+e^- \rightarrow \Upsilon(4S) \rightarrow B\bar{B}$ in an entangled quantum state. Because of flavor mixing, decays of two B^0 or \bar{B}^0 mesons are observed. If CP is violated in mixing, $\mathcal{P} \neq \bar{\mathcal{P}}$ and a different number of $B^0\bar{B}^0$ events with respect to \bar{B}^0B^0 is expected. The asymmetry is measured by selecting flavor tagged final states f , for which the decay $B^0 \rightarrow f$ is allowed and the decay $\bar{B}^0 \rightarrow f$ is forbidden. Inclusive semileptonic decays $B^0 \rightarrow \ell^+\nu_\ell X$ have been used in the past, due to the large branching fraction and high selection efficiency (unless the contrary is explicitly stated, we always imply charge conjugated processes; “lepton” ℓ means either electron or muon). Assuming CPT symmetry for semileptonic decays [$\Gamma(B^0 \rightarrow \ell^+\nu_\ell X) = \Gamma(\bar{B}^0 \rightarrow \ell^-\bar{\nu}_\ell \bar{X})$], the observed asymmetry is directly related to CP violation in mixing:

$$\frac{\mathcal{N}(\ell^+\ell^+) - \mathcal{N}(\ell^-\ell^-)}{\mathcal{N}(\ell^+\ell^+) + \mathcal{N}(\ell^-\ell^-)} = \mathcal{A}_{CP} \quad (8)$$

where $\mathcal{N}(\ell^\pm\ell^\pm)$ is the efficiency-corrected number of equal charge dilepton events after background subtraction.

Published results from CLEO [5] and the B factory experiments of Belle [6] and BABAR [7,8], based on the analysis of dilepton events, are consistent with the SM expectation. The $D0$ Collaboration [9], using a dimuon sample, obtained a more precise measurement, which however includes contributions from both B^0 and B_s^0 mixing. They observe a deviation larger than three standard deviations from the SM expectation. Measurements based on the reconstruction of $\bar{B}_s^0 \rightarrow D_s^{(*)+} \ell^-\bar{\nu}_\ell$ decays [10,11] and of $\bar{B}^0 \rightarrow D^{(*)+} \ell^-\bar{\nu}_\ell$ decays [12,13] are compatible both with the SM and with $D0$.

The dilepton measurements benefit from the large number of events that can be selected at B factories or at hadron colliders. However, they rely on the use of control samples to subtract the charge-asymmetric background originating from hadrons wrongly identified as leptons or leptons from light hadron decays, and to compute the charge-dependent lepton identification asymmetry that may produce a false signal. The systematic uncertainties associated with the corrections for these effects constitute a severe limitation of the precision of the measurements. Particularly obnoxious is the case when a lepton from a direct B semileptonic decay is combined with a lepton of equal charge from a charm meson produced in the decay of the other B . As the mixing probability is rather low, this background process is enhanced with respect to the signal, so that stringent kinematic selections need to be applied. Authors of [14] suggest that at least a part of the $D0$ dilepton discrepancy could be due to charm decays.

Herein we present in detail a measurement which overcomes these difficulties with a new approach. To reduce the background dilution from B^+B^- or from light quark events, we reconstruct $\bar{B}^0 \rightarrow D^{*+} \ell^-\bar{\nu}_\ell$ decays with a very

efficient selection using only the charged lepton and the low-momentum pion (π_s) from the $D^{*+} \rightarrow D^0 \pi_s$ decay. A state decaying as a B^0 (\bar{B}^0) meson produces $\ell^+ \pi_s^-$ ($\ell^- \pi_s^+$). We use charged kaons from decays of the other B^0 to tag its flavor (K_T). Kaons are mostly produced in the Cabibbo-favored (CF) process $B^0 \rightarrow \bar{D} X$, $\bar{D} \rightarrow K^+ X'$, so that a state decaying as a B^0 (\bar{B}^0) meson results most often in a K^+ (K^-). If mixing takes place, the ℓ and the K will have the same charge. Kaons produced in association with the $\ell \pi_s$ pair are used to measure the large instrumental asymmetry in kaon identification.

The observed asymmetry between the number of positive-charge and negative-charge leptons can be approximated as

$$A_\ell \simeq \mathcal{A}_{r\ell} + \mathcal{A}_{CP} \cdot \chi_d, \quad (9)$$

where $\chi_d = 0.1862 \pm 0.0023$ [1] is the integrated mixing probability for B^0 mesons, and $\mathcal{A}_{r\ell}$ is the charge asymmetry in the reconstruction of $\bar{B}^0 \rightarrow D^{*+} \ell^- \bar{\nu}_\ell$ decays.

With the same approximations as before, the observed asymmetry in the rate of kaon-tagged mixed events is

$$\begin{aligned} A_T &= \frac{N(\ell^+ K_T^+) - N(\ell^- K_T^-)}{N(\ell^+ K_T^+) + N(\ell^- K_T^-)} \\ &\simeq \mathcal{A}_{r\ell} + \mathcal{A}_K + \mathcal{A}_{CP}, \end{aligned} \quad (10)$$

where \mathcal{A}_K is the charge asymmetry in kaon reconstruction. A kaon with the same charge as the ℓ might also come from the CF decays of the D^0 meson produced with the lepton from the partially reconstructed side (K_R). The asymmetry observed for these events is

$$A_R = \frac{N(\ell^+ K_R^+) - N(\ell^- K_R^-)}{N(\ell^+ K_R^+) + N(\ell^- K_R^-)} \simeq \mathcal{A}_{r\ell} + \mathcal{A}_K + \mathcal{A}_{CP} \cdot \chi_d. \quad (11)$$

Equations (9), (10), and (11), defining quantities computed in terms of the observed number of events integrated over time, can be inverted to extract \mathcal{A}_{CP} and the detector induced asymmetries. It is not possible to distinguish a K_T from a K_R in each event. They are separated on a statistical basis, using kinematic features and proper-time difference information.

III. THE BABAR DETECTOR

A detailed description of the BABAR detector and the algorithms used for charged and neutral particle reconstruction and identification is provided elsewhere [15,16]. A brief summary is given here. The momentum of charged particles is measured by the tracking system, which consists of a silicon vertex tracker (SVT) and a drift chamber (DCH) in a 1.5 T magnetic field. The positions of points along the trajectories of charged particles measured

with the SVT are used for vertex reconstruction and for measuring the momentum of charged particles, including those particles with low transverse momentum that do not reach the DCH due to the bending in the magnetic field. The energy loss in the SVT is used to discriminate low-momentum pions from electrons.

Higher-energy electrons are identified from the ratio of the energy of their associated shower in the electromagnetic calorimeter (EMC) to their momentum, the transverse profile of the shower, the energy loss in the DCH, and the information from the Cherenkov detector (DIRC). The electron identification efficiency is 93%, and the misidentification rate for pions and kaons is less than 1%.

Muons are identified on the basis of the energy deposited in the EMC and the penetration in the instrumented flux return (IFR) of the superconducting coil, which contains resistive plate chambers and limited streamer tubes interspersed with iron. Muon candidates compatible with the kaon hypothesis in the DIRC are rejected. The muon identification efficiency is about 80%, and the misidentification rate for pions and kaons is $\sim 3\%$.

We select kaons from charged particles with momenta larger than 0.2 GeV/c using a standard algorithm which combines DIRC information with the measurements of the energy losses in the SVT and DCH. True kaons are identified with $\sim 85\%$ efficiency and a $\sim 3\%$ pion misidentification rate.

IV. EVENT SELECTION

The data sample used in this analysis consists of 468 million $B\bar{B}$ pairs, corresponding to an integrated luminosity of 425.7 fb^{-1} collected at the $\Upsilon(4S)$ resonance (on-resonance) and 45 fb^{-1} collected 40 MeV below the resonance (off-resonance) by the BABAR detector [17]. The off-resonance events are used to describe the non- $B\bar{B}$ (continuum) background. A simulated sample of $B\bar{B}$ events with integrated luminosity equivalent to approximately three times the size of the data sample, based on EVTGEN [18] and GEANT4 [19] with full detector response and event reconstruction, is used to test the analysis procedure.

We preselect a sample of hadronic events with at least four charged particles. To reduce continuum background we require the ratio of the second to the zeroth order Fox-Wolfram variables [20] to be less than 0.6. We then select a sample of partially reconstructed B mesons in the channel $\bar{B}^0 \rightarrow D^{*+} X \ell^- \bar{\nu}_\ell$, by retaining events containing a charged lepton ($\ell = e, \mu$) and a low-momentum pion (soft pion, π_s^+) from the decay $D^{*+} \rightarrow D^0 \pi_s^+$. The lepton momentum must be in the range $1.4 < p_{\ell^-} < 2.3 \text{ GeV}/c$ and the soft pion candidate must satisfy $60 < p_{\pi_s^+} < 190 \text{ MeV}/c$. Throughout this paper the momentum, energy and direction of all particles are determined in the e^+e^- rest frame. The two tracks must be consistent with originating

from a common vertex, constrained to the beam-spot in the plane transverse to the e^+e^- collision axis. Finally, we combine p_{ℓ^-} , $p_{\pi_s^+}$ and the probability from the vertex fit into a likelihood ratio variable (η). A cut on η is optimized to reject background from other $B\bar{B}$ events. If more than one combination is found in an event, we keep the one with the largest value of η .

The squared missing mass is

$$\mathcal{M}_{\text{miss}}^2 \equiv (E_{\text{beam}} - E_{D^*} - E_{\ell})^2 - (\mathbf{p}_{D^*} + \mathbf{p}_{\ell})^2, \quad (12)$$

where we neglect the momentum of the B^0 ($p_B \approx 340 \text{ MeV}/c$) and identify the B^0 energy with the beam energy E_{beam} in the e^+e^- center-of-mass frame; E_{ℓ} and \mathbf{p}_{ℓ} are the energy and momentum of the lepton and \mathbf{p}_{D^*} is the estimated momentum of the D^* . As a consequence of the limited phase space available in the D^{*+} decay, the soft pion is emitted in a direction close to that of the D^{*+} and a strong correlation holds between the energy of the two particles in the B^0 center-of-mass frame. The D^{*+} four-momentum can, therefore, be estimated by approximating its direction as that of the soft pion, and parametrizing its momentum as a linear function of the soft-pion momentum using simulated events. We select pairs of tracks with opposite charge for the signal ($\ell^\mp \pi_s^\pm$) and we use same-charge pairs ($\ell^\pm \pi_s^\pm$) for background studies.

Several processes where D^{*+} and ℓ^- originate from the same B -meson produce a peak near zero in the $\mathcal{M}_{\text{miss}}^2$ distribution. The signal consists of (a) $\bar{B}^0 \rightarrow D^{*+} \ell^- \bar{\nu}_\ell$ decays (primary); (b) $\bar{B}^0 \rightarrow D^{*+} (n\pi) \ell^- \bar{\nu}_\ell$ (D^{**}), and (c) $\bar{B}^0 \rightarrow D^{*+} \tau^- \bar{\nu}_\tau$, $\tau^- \rightarrow \ell^- \bar{\nu}_\ell \nu_\tau$. The main source of peaking background is due to charged- B decays to resonant or nonresonant charm excitations, $B^+ \rightarrow D^{*+} (n\pi) \ell^- \bar{\nu}_\ell$, or to τ leptons, and $B \rightarrow D^{*+} h^- X$, where the hadron ($h = \pi, K, D$) is erroneously identified as, or decays to, a charged lepton. We also include radiative events, where photons with energy above 1 MeV are emitted by any charged particle, as described in the simulation by PHOTOS [21]. We define the signal region $\mathcal{M}_{\text{miss}}^2 > -2 \text{ GeV}^2/c^4$, and the sideband $-10 < \mathcal{M}_{\text{miss}}^2 < -4 \text{ GeV}^2/c^4$.

Continuum events and random combinations of a low-momentum pion and an opposite-charge lepton from combinatorial $B\bar{B}$ events contribute to the nonpeaking background. We determine the number of signal events in the sample with a minimum- χ^2 fit to the $\mathcal{M}_{\text{miss}}^2$ distribution in the interval $-10 < \mathcal{M}_{\text{miss}}^2 < 2.5 \text{ GeV}^2/c^4$. In the fit, the continuum contribution is obtained from off-peak events, normalized by the on-peak to off-peak luminosity ratio; the other contributions are taken from the simulation. The number of events from combinatorial $B\bar{B}$ background, primary decays and D^{**} [(a) and (b) categories described previously] is allowed to vary in the fit, while the other peaking contributions are fixed to the simulation expectations (few percent). The number of B^0 mesons in

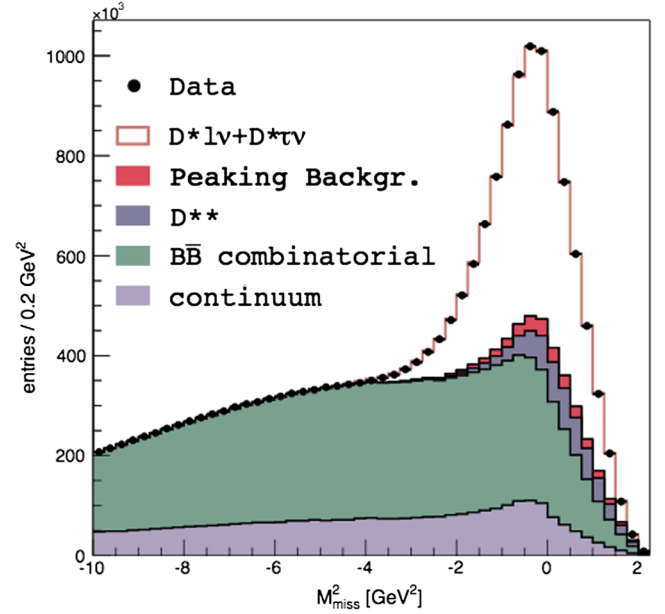


FIG. 1. $\mathcal{M}_{\text{miss}}^2$ distribution for the selected events. The data are represented by the points with error bars. The fitted contributions from $\bar{B}^0 \rightarrow D^{*+} \ell^- \bar{\nu}_\ell$ plus $\bar{B}^0 \rightarrow D^{*+} \tau^- \bar{\nu}_\tau$, peaking background, D^{**} events (1/3 from \bar{B}^0 and 2/3 from B^+ decays), $B\bar{B}$ combinatorial, and rescaled off-peak events are shown (see text for details).

the sample is then obtained assuming that 2/3 of the fitted number of D^{**} events are produced by B^+ decays, as suggested by simple isospin considerations. We find a total of $(5.945 \pm 0.007) \times 10^6$ signal events, where the uncertainty is only statistical. In the full range signal events account for about 30% of the sample and continuum background for about 15%. The result of the fit is shown in Fig. 1.

V. KAON TAG

We indicate with K_R (K_T) kaons produced from the decay of the D^0 from the partially reconstructed B^0 (B_R), or in any step of the decay of the other B (B_T). We exploit the relation between the charge of the lepton and that of the K_T to define an event as “mixed” or “unmixed”. When an oscillation takes place, and the two B^0 mesons in the event have the same flavor at decay time, a K_T from a CF decay has the same charge as the ℓ . Equal-charge combinations are also observed from Cabibbo-suppressed (CS) K_T production in unmixed events, and from CF K_R production. Unmixed CF K_T , mixed CS K_T , and CS K_R result in opposite-charge combinations. Other charged particles wrongly identified as kaons contribute both to equal and opposite charge events with comparable rates.

We distinguish K_T from K_R using proper-time difference information. We define $\Delta Z = Z_{\text{rec}} - Z_{\text{tag}}$, where Z_{rec} is the projection along the beam direction of the B_R decay point, and Z_{tag} is the projection along the same direction of the

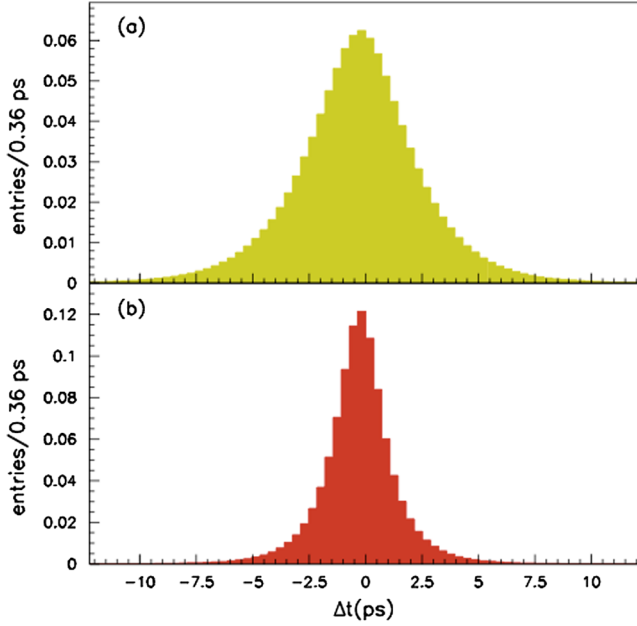


FIG. 2. Δt distributions for (a) K_T and for (b) K_R , as predicted by the simulation.

intersection of the K track trajectory with the beam-spot. In the boost approximation [22] we measure the proper-time difference between the two B meson decays using the relation $\Delta t = \Delta Z/(\beta\gamma c)$, where the parameters β , γ express the Lorentz boost from the laboratory to the $\Upsilon(4S)$ rest frame. We reject events if the uncertainty $\sigma(\Delta t)$ exceeds 3 ps.

Due to the short lifetime and small boost of the D^0 meson, small values of Δt are expected for the K_R . Much larger values are instead expected for CF mixed K_T , due to the long period of the B^0 oscillation. Figure 2 shows the Δt distributions for K_T and K_R events, as obtained from the simulation. To improve the separation between K_T and K_R , we also exploit kinematics. In the rest frame of the B^0 , the ℓ and the D^{*+} are emitted at large angles. Therefore the angle $\theta_{\ell K}$ between the ℓ and the K_R has values close to π , and $\cos \theta_{\ell K}$ close to -1 . The corresponding distribution for K_T is instead uniform, as shown in Fig. 3.

In about 20% of the cases, our events contain more than one kaon: most often we find both a K_T and a K_R candidate. As these two carry different information, we accept multiple candidate events. Using several simulated pseudoexperiments, we assess the effect of this choice on the statistical uncertainty.

VI. EXTRACTION OF Δ_{CP}

The measurement proceeds in two stages.

First we measure the sample composition of the eight tagged samples grouped by lepton kind, lepton charge and K charge, with the fit to $\mathcal{M}_{\text{miss}}^2$ previously described. We also fit the four inclusive lepton samples to determine the charge asymmetries at the reconstruction stage [see

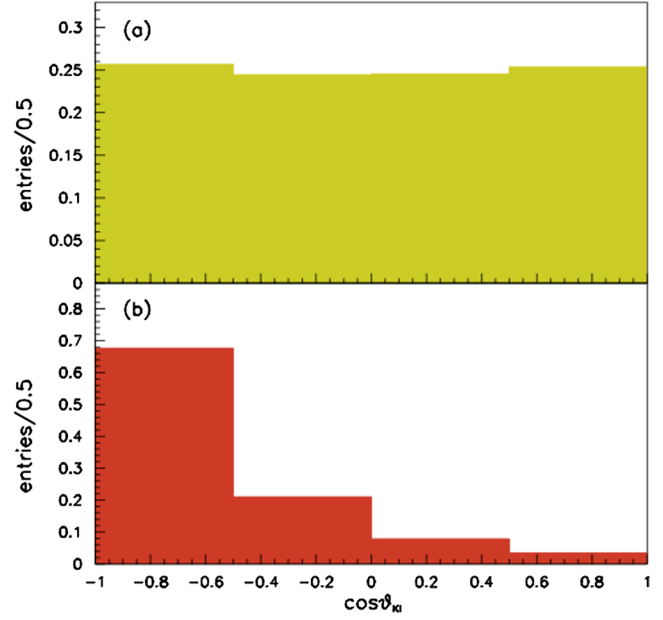


FIG. 3. $\cos(\theta_{\ell K})$ distributions for (a) K_T and for (b) K_R , as predicted by the simulation.

Eq. (9)]. At this point of the analysis we use the total number of collected events.

The results of the first stage are used in the second stage, where we fit simultaneously the $\cos \theta_{\ell K}$ and Δt distributions in the eight tagged samples.

The Δt distributions for $B\bar{B}$, BB and $\bar{B}\bar{B}$ events are parametrized as the convolutions of the theoretical distributions $\mathcal{F}_i(\Delta t'|\vec{\Theta})$ with the resolution function $\mathcal{R}(\Delta t, \Delta t')$: $\mathcal{G}_i(\Delta t) = \int_{-\infty}^{+\infty} \mathcal{F}_i(\Delta t'|\vec{\Theta})\mathcal{R}(\Delta t, \Delta t')d(\Delta t')$, where $\Delta t'$ is the actual difference between the times of decay of the two mesons and $\vec{\Theta}$ is the vector of the physical parameters. The decays of the B^+ mesons are parametrized by an exponential function, $\mathcal{F}_{B^+} = \Gamma_+ e^{-|\Gamma_+ \Delta t'|}$, where the B^+ decay width is the inverse of the lifetime $\Gamma_+^{-1} = \tau_+ = 1.641 \pm 0.008$ ps [1]. According to Ref. [23], the decays of the B^0 mesons are described by the following expressions:

$$\begin{aligned} \mathcal{F}_{\bar{B}^0 B^0}(\Delta t') = \mathcal{E}(\Delta t') & \left[\left(1 + \left| \frac{q}{p} \right|^2 r^2 \right) \cosh(\Delta\Gamma\Delta t'/2) \right. \\ & + \left(1 - \left| \frac{q}{p} \right|^2 r^2 \right) \cos(\Delta m\Delta t') \\ & \left. - \left| \frac{q}{p} \right| (b+c) \sin(\Delta m\Delta t') \right] \end{aligned} \quad (13)$$

$$\begin{aligned} \mathcal{F}_{B^0 \bar{B}^0}(\Delta t') = \mathcal{E}(\Delta t') & \left[\left(1 + \left| \frac{p}{q} \right|^2 r^2 \right) \cosh(\Delta\Gamma\Delta t'/2) \right. \\ & + \left(1 - \left| \frac{p}{q} \right|^2 r^2 \right) \cos(\Delta m\Delta t') \\ & \left. + \left| \frac{p}{q} \right| (b-c) \sin(\Delta m\Delta t') \right] \end{aligned} \quad (14)$$

$$\begin{aligned} \mathcal{F}_{\bar{B}^0 \bar{B}^0}(\Delta t') &= \mathcal{E}(\Delta t') \left[\left(1 + \left| \frac{p}{q} \right|^2 r'^2 \right) \cosh(\Delta \Gamma \Delta t' / 2) \right. \\ &\quad - \left(1 - \left| \frac{p}{q} \right|^2 r'^2 \right) \cos(\Delta m \Delta t') \\ &\quad \left. - \left| \frac{p}{q} \right| (b - c) \sin(\Delta m \Delta t') \right] \left| \frac{q}{p} \right|^2 \end{aligned} \quad (15)$$

$$\begin{aligned} \mathcal{F}_{B^0 B^0}(\Delta t') &= \mathcal{E}(\Delta t') \left[\left(1 + \left| \frac{q}{p} \right|^2 r'^2 \right) \cosh(\Delta \Gamma \Delta t' / 2) \right. \\ &\quad - \left(1 - \left| \frac{q}{p} \right|^2 r'^2 \right) \cos(\Delta m \Delta t') \\ &\quad \left. + \left| \frac{q}{p} \right| (b + c) \sin(\Delta m \Delta t') \right] \left| \frac{p}{q} \right|^2 \\ \mathcal{E}(\Delta t') &= \frac{\Gamma_0}{2(1 + r'^2)} e^{-\Gamma_0 |\Delta t'|}, \end{aligned} \quad (16)$$

where the first index refers to the flavor of the B_R and the second index to that of the B_T . In Eqs. (13)–(16), $\Gamma_0 = \tau_{B^0}^{-1}$ is the average width of the two B^0 mass eigenstates, Δm and $\Delta \Gamma$ are respectively their mass and width differences, r' is a parameter resulting from the interference of CF and doubly Cabibbo-suppressed (DCS) decays on the B_T side, and b and c are two parameters expressing the CP violation arising from that interference. In the Standard Model the value of r' is rather small, $\mathcal{O}(1\%)$, $b = 2r' \sin(2\beta + \gamma) \cos \delta'$, and $c = -2r' \cos(2\beta + \gamma) \sin \delta'$, where β and γ are angles of the unitary triangle [24], and δ' is a strong phase. Besides $|q/p|$, also Δm , τ_{B^0} , $\sin(2\beta + \gamma)$, b , and c are determined as effective parameters to reduce the systematic uncertainty. The value of $\Delta \Gamma$ is fixed to zero, and then varied within its allowed range [1] when computing the systematic uncertainty. Neglecting the tiny contribution from DCS decays, the main contribution to the asymmetry is time independent and due to the normalization factors in Eqs. (15) and (16).

When the K_T comes from the decay of the B^0 meson to a CP eigenstate [as, for instance $B^0 \rightarrow D^{(*)} D^{(*)}$], a different expression applies:

$$\begin{aligned} \mathcal{F}_{CP}(\Delta t') &= \frac{\Gamma_0}{4} e^{-\Gamma_0 |\Delta t'|} [1 \pm S \sin(\Delta m \Delta t') \\ &\quad \pm C \cos(\Delta m \Delta t')], \end{aligned} \quad (17)$$

where the sign plus is used if the B_R decays as a B^0 and the sign minus otherwise. This sample contains several components and is strongly biased by the selection cuts; therefore we take the values of S and C , and the fraction of these events in each sample (about 1%) from the simulation.

The resolution function $\mathcal{R}(\Delta t, \Delta t')$ accounts for the uncertainties in the measurement of Δt , for the effect of the boost approximation, and for the displacement of the K_T production point from the B_T decay position due to the motion of the charm meson. It consists of the superposition of several Gaussian functions convolved with exponentials.

We determine Δ_{CP} with two different inputs for $\mathcal{G}_{K_R}(\Delta t)$, describing the Δt distribution for K_R events, and take the mean value of the two determinations as the nominal result. As first input, we use the distribution obtained from a high purity selection of K_R events on data, $\mathcal{G}_{K_R}^{\text{Data}}(\Delta t)_{HP}$. As second input, we use the distribution for K_R events as predicted by the simulation, $\mathcal{G}_{K_R}^{\text{MC}}(\Delta t)$, corrected using Eq. (18):

$$\mathcal{G}_{K_R}^{\text{Data}}(\Delta t) = \mathcal{G}_{K_R}^{\text{MC}}(\Delta t) \times \left(\frac{\mathcal{G}_{K_R}^{\text{Data}}(\Delta t)}{\mathcal{G}_{K_R}^{\text{MC}}(\Delta t)} \right)_{HP}. \quad (18)$$

To select the high purity K_R sample, we require the lepton and the kaon to have the same charge. As discussed above, this sample consists of about 75% genuine K_R , where the residual number of events with a K_T is mostly due to mixing. Therefore we select events with a second high-momentum lepton, with charge opposite to that of the first lepton. According to the simulation, this raises the K_R purity in the sample to about 87%. Finally, we use topological variables, correlating the kaon momentum-vector to those of the two leptons, to raise the K_R purity in the sample to about 95%.

Due to the large number of events, the fit complexity, and the high number of floated parameters, the time needed for an unbinned fit to reach convergence is too large; therefore we perform a binned maximum likelihood fit. Events belonging to each of the eight categories are grouped into 100 Δt bins; 25 $\sigma(\Delta t)$ bins; 4 $\cos \theta_{\ell, K}$ bins; and 5 $\mathcal{M}_{\text{miss}}^2$ bins. We further split the data into five bins of K momentum, p_K , to account for the dependencies of several parameters, describing the Δt resolution function, the $\cos(\theta_{\ell, K})$ distributions, the fractions of K_T events, etc., observed in the simulation.

Accounting for events with wrong flavor assignment and K_R events, the peaking B^0 contributions to the equal and opposite charge samples in each bin j are

$$\begin{aligned} \mathcal{G}_{\ell^+ K^+}^{B^0}(j) &= (1 + \mathcal{A}_{r\ell})(1 + \mathcal{A}_K) \{ (1 - f_{K_R}^{++}) [(1 - \omega^+) \mathcal{G}_{B^0 B^0}(j) + \omega^- \mathcal{G}_{B^0 \bar{B}^0}(j)] + f_{K_R}^{++} (1 - \omega'^+) \mathcal{G}_{K_R}(j) (1 + \chi_d \mathcal{A}_{CP}) \} \\ \mathcal{G}_{\ell^- K^-}^{B^0}(j) &= (1 - \mathcal{A}_{r\ell})(1 - \mathcal{A}_K) \{ (1 - f_{K_R}^{--}) [(1 - \omega^-) \mathcal{G}_{\bar{B}^0 \bar{B}^0}(j) + \omega^+ \mathcal{G}_{\bar{B}^0 B^0}(j)] + f_{K_R}^{--} (1 - \omega'^-) \mathcal{G}_{K_R}(j) (1 - \chi_d \mathcal{A}_{CP}) \} \\ \mathcal{G}_{\ell^+ K^-}^{B^0}(j) &= (1 + \mathcal{A}_{r\ell})(1 - \mathcal{A}_K) \{ (1 - f_{K_R}^{+-}) [(1 - \omega^-) \mathcal{G}_{B^0 \bar{B}^0}(j) + \omega^+ \mathcal{G}_{B^0 B^0}(j)] + f_{K_R}^{+-} \omega'^+ \mathcal{G}_{K_R}(j) (1 + \chi_d \mathcal{A}_{CP}) \} \\ \mathcal{G}_{\ell^- K^+}^{B^0}(j) &= (1 - \mathcal{A}_{r\ell})(1 + \mathcal{A}_K) \{ (1 - f_{K_R}^{-+}) [(1 - \omega^+) \mathcal{G}_{\bar{B}^0 B^0}(j) + \omega^- \mathcal{G}_{\bar{B}^0 \bar{B}^0}(j)] + f_{K_R}^{-+} \omega'^- \mathcal{G}_{K_R}(j) (1 - \chi_d \mathcal{A}_{CP}) \} \end{aligned} \quad (19)$$

where the probability density functions (PDFs) $\mathcal{G}_{B^0 B^0}(\Delta t)$, $\mathcal{G}_{B^0 \bar{B}^0}(\Delta t)$, $\mathcal{G}_{\bar{B}^0 B^0}(\Delta t)$ and $\mathcal{G}_{\bar{B}^0 \bar{B}^0}(\Delta t)$ are the convolutions of the theoretical distributions in Eqs. (13)–(16) with the resolution function. The reconstruction asymmetries $\mathcal{A}_{r\ell}$ are determined separately for the e and μ samples. Wrong-flavor assignments are described by the probabilities ω^\pm for B_T and ω'^\pm for B_R . They are different because K_T 's come from a mixture of D mesons, while K_R 's are produced by D^0 decays only. The parameters $f_{K_R}^{\pm\pm}(p_K)$ describe the fractions of K_R tags in each sample as a function of the kaon momentum. Due to the different charge asymmetry of the K_T and the K_R events [see Eqs. (10) and (11)], the fitted values of $f_{K_R}^{\pm\pm}(p_K)$ and $|q/p|$ are strongly correlated. The $f_{K_R}^{\pm\pm}(p_K)$ fractions can be factorized as

$$f_{K_R}^{\pm\pm}(|q/p|) = f_{K_R}^{\pm\pm}(|q/p| = 1) \times g^{\pm\pm}(|q/p|) \quad (20)$$

where the $f_{K_R}^{\pm\pm}(|q/p| = 1)$ parameters are left free in the fit and $g^{\pm\pm}(|q/p|)$ are analytical functions. In order to limit the number of free parameters in the fit, the fractions of K_R events in the B^+ sample are computed from the corresponding fractions in the B^0 samples:

$$f_{K_R}^{\pm\pm}(B^+) = f_{K_R}^{\pm\pm}(|q/p| = 1) \times R^{\pm\pm} \quad (21)$$

where $R^{\pm\pm}$ are correction factors obtained from the simulation.

The combinatorial background consists of B^+ and \bar{B}^0 decays with comparable contributions. A non-negligible fraction of \bar{B}^0 combinatorial events is obtained when the lepton in $B \rightarrow D^* X \ell \nu$ decay is combined with a soft pion from the decay of a tag-side $D^{*\pm}$. As the two particles must have opposite charges, the fraction of mixed events in the \bar{B}^0 combinatorial background is larger than for peaking events. In the simulation we find that the effective mixing rate of the combinatorial events depends linearly on the kaon momentum according to the relation

$$\chi_d^{\text{comb}} = \chi_0^{\text{comb}}(a + b \cdot p_K), \quad (22)$$

where

$$\chi_0^{\text{comb}} = \frac{x_{\text{comb}}^2}{2(1 + x_{\text{comb}}^2)} \quad (23)$$

and $x_{\text{comb}} = \Delta m^{\text{comb}} \tau_{B^0}^{\text{comb}}$. In this expression, Δm^{comb} and $\tau_{B^0}^{\text{comb}}$ are the mass difference and lifetime measured in combinatorial events. To account for this effect, we use for the \bar{B}^0 combinatorial background the same expressions as for the signal [see Eq. (19)], with the replacements

$$\begin{aligned} \mathcal{G}_{\bar{B}^0 \bar{B}^0}^{\text{comb}} &= \mathcal{G}_{\bar{B}^0 \bar{B}^0} \frac{\chi_d^{\text{comb}}}{\chi_0^{\text{comb}}}, \\ \mathcal{G}_{B^0 B^0}^{\text{comb}} &= \mathcal{G}_{B^0 B^0} \frac{\chi_d^{\text{comb}}}{\chi_0^{\text{comb}}}, \\ \mathcal{G}_{\bar{B}^0 B^0}^{\text{comb}} &= \mathcal{G}_{\bar{B}^0 B^0} \frac{1 - \chi_d^{\text{comb}}}{1 - \chi_0^{\text{comb}}}, \\ \mathcal{G}_{B^0 \bar{B}^0}^{\text{comb}} &= \mathcal{G}_{B^0 \bar{B}^0} \frac{1 - \chi_d^{\text{comb}}}{1 - \chi_0^{\text{comb}}}. \end{aligned} \quad (24)$$

The parameters a and b in Eq. (22), Δm^{comb} and $\tau_{B^0}^{\text{comb}}$ are determined in the fit.

The probabilities to assign a wrong flavor to B_T in the combinatorial sample are found to be different in mixed and unmixed events.

Different sets of parameters are used for peaking and for combinatorial events, including lifetimes, frequencies of \bar{B}^0 oscillation, and detector-related asymmetries, whereas the same value of $|q/p|$ is used. For B^+ combinatorial events, the same PDFs as for peaking B^+ background are employed, with different sets of parameters.

The distribution $\mathcal{G}_{\text{cont}}(\Delta t)$ of continuum events is represented by a decaying exponential, convolved with a resolution function similar to that used for B events. The effective lifetime and resolution parameters are determined by fitting simultaneously the off-peak data.

We rely on the simulation to parametrize the $\cos \theta_{\ell K}$ distributions. The individual $\cos \theta_{\ell K}$ shapes for the eight $B\bar{B}$ tagged samples are obtained from the histograms of the corresponding simulated distributions, separately for K_T and K_R events, whereas we interpolate off-peak data to describe the continuum.

The normalized Δt distributions for each tagged sample are then expressed as the sum of the predicted contributions from peaking, $B\bar{B}$ combinatorial, and continuum background events:

$$\begin{aligned} \mathcal{F}^{\ell K}(\Delta t, \sigma_{\Delta t}, \mathcal{M}_{\text{miss}}^2, \cos \theta_{\ell K}, p_K | \tau_{B^0}, \Delta m, |q/p|) \\ = (1 - f_{B^+}(\mathcal{M}_{\text{miss}}^2) - f_{CP}(\mathcal{M}_{\text{miss}}^2) - f_{\text{comb}}(\mathcal{M}_{\text{miss}}^2) - f_{\text{cont}}(\mathcal{M}_{\text{miss}}^2)) \mathcal{G}_{\ell K}^{B^0}(\Delta t, \sigma_{\Delta t}, \cos \theta_{\ell K}, p_K) \\ + f_{B^+}(\mathcal{M}_{\text{miss}}^2) \mathcal{G}_{\ell K}^{B^+}(\Delta t, \sigma_{\Delta t}, \cos \theta_{\ell K}, p_K) + f_{CP}(\mathcal{M}_{\text{miss}}^2) \mathcal{G}_{\ell K}^{CP}(\Delta t, \sigma_{\Delta t}, \cos \theta_{\ell K}, p_K) \\ + f_{\text{comb}}^0(\mathcal{M}_{\text{miss}}^2) \mathcal{G}_{\ell K}^{B^0 \text{comb}}(\Delta t, \sigma_{\Delta t}, \cos \theta_{\ell K}, p_K) + f_{\text{comb}}^+(\mathcal{M}_{\text{miss}}^2) \mathcal{G}_{\ell K}^{B^+ \text{comb}}(\Delta t, \sigma_{\Delta t}, \cos \theta_{\ell K}, p_K) \\ + f_{\text{cont}}(\mathcal{M}_{\text{miss}}^2) \mathcal{G}_{\ell K}^{\text{cont}}(\Delta t, \sigma_{\Delta t}, \cos \theta_{\ell K}, p_K) \end{aligned} \quad (25)$$

where the fractions of peaking B^+ (f_{B^+}), CP eigenstates (f_{CP}), combinatorial $B\bar{B}$ (f_{comb}), and continuum (f_{cont}) events in each $\mathcal{M}_{\text{miss}}^2$ interval are taken from the results of the first stage. The fraction of B^0 (f_{comb}^0) and of B^+ events ($f_{\text{comb}}^+ = f_{\text{comb}} - f_{\text{comb}}^0$) in the combinatorial background have been determined from a simulation. The functions $\mathcal{G}_{\ell K}^{B^0}(j)$ for peaking B^0 events are defined in Eq. (19); the functions $\mathcal{G}_{\ell K}^{B^+}(j)$, $\mathcal{G}_{\ell K}^{CP}(j)$, $\mathcal{G}_{\ell K}^{B^0\text{comb}}(j)$, $\mathcal{G}_{\ell K}^{B^+\text{comb}}(j)$ and $\mathcal{G}_{\ell K}^{\text{cont}}(j)$ are the corresponding PDFs for the other samples.

For a sample of B^0 signal events tagged by a kaon from the B_T meson decay, the expected fraction P_m^{exp} of mixed events in each p_K bin depends on Δm , τ_{B^0} , and ω^\pm , and reads

$$P_m^{\text{exp}} = \frac{\mathcal{G}_{\ell^+K^+}^{B_T^0} + \mathcal{G}_{\ell^-K^-}^{B_T^0}}{\mathcal{G}_{\ell^+K^+}^{B_T^0} + \mathcal{G}_{\ell^-K^-}^{B_T^0} + \mathcal{G}_{\ell^+K^-}^{B_T^0} + \mathcal{G}_{\ell^-K^+}^{B_T^0}}, \quad (26)$$

where the functions $\mathcal{G}_{\ell K}^{B_T^0}$ are obtained from Eq. (19) taking into account only the contributions from B_T^0 events.

We estimate this fraction by multiplying the likelihood by the binomial factor

$$C_m^{B_T^0} = \frac{N!}{N_m!N_u!} (P_m^{\text{exp}})^{N_m} (1 - P_m^{\text{exp}})^{N_u}, \quad (27)$$

where N_m and N_u are the number of mixed and unmixed events, respectively, in a given p_K bin for each subsample. These are obtained as the sums of the numbers of mixed events tagged by a kaon of a given charge,

$$N_m = N_{m,K^+} + N_{m,K^-} \quad (28)$$

$$N_u = N_{u,K^+} + N_{u,K^-}. \quad (29)$$

Finally, $N = N_m + N_u$.

The corresponding value of $P_{m,\text{comb}}^{\text{exp}}$ for the sample of B^0 combinatorial events tagged by a kaon from the B_T meson decay depends on Δm^{comb} , $\tau_{B^0}^{\text{comb}}$, and the wrong flavor assignment probability for the mixed and unmixed subsamples.

For a sample of B^0 events tagged by a kaon from the B_T meson decay, the expected fraction of mixed and unmixed events, tagged by a positive charge kaon, depends on \mathcal{A}_{CP} and the detector charge asymmetries. For the B^0 signal sample this fraction reads

$$P_{m(u),K^+}^{\text{exp}} = \frac{\mathcal{G}_{\ell^+(\ell^-)K^+}^{B_T^0}}{\mathcal{G}_{\ell^+(\ell^-)K^+}^{B_T^0} + \mathcal{G}_{\ell^-(\ell^+)K^-}^{B_T^0}}. \quad (30)$$

We estimate this quantity by multiplying the likelihood by the binomial factor

$$C_{m(u),K^+}^{B_T^0} = \frac{N_{m(u)}!}{N_{m(u),K^+}!N_{m(u),K^-}!} \times (P_{m(u),K^+}^{\text{exp}})^{N_{m(u),K^+}} \times (1 - P_{m(u),K^+}^{\text{exp}})^{N_{m(u),K^-}}. \quad (31)$$

For a sample of B^0 events tagged by a kaon from the B_R meson decay, the fraction of mixed events depends on ω'^\pm . The fraction of mixed and unmixed events, tagged by a positive charge kaon, depends on the detector charge asymmetries and on \mathcal{A}_{CP} . Analogously, the corresponding fractions for a sample of B^+ events tagged by a kaon from the B_T or B_R meson decay give information on the detector charge asymmetries.

The same values of \mathcal{A}_{CP} and \mathcal{A}_K are shared between signal and combinatorial B^0 samples. The values of P_m^{exp} and $P_{m(u),K^+}^{\text{exp}}$ for all the subsamples are obtained from the ratio of integrals of the corresponding observed PDFs.

We maximize the likelihood

$$\begin{aligned} \mathcal{L} = & \left(\prod_{i=1}^{N_{m,K^+}} \mathcal{F}_i^{\ell^+K^+} \right) \left(\prod_{j=1}^{N_{m,K^-}} \mathcal{F}_j^{\ell^-K^-} \right) \\ & \times \left(\prod_{m=1}^{N_{u,K^+}} \mathcal{F}_m^{\ell^-K^+} \right) \left(\prod_{n=1}^{N_{u,K^-}} \mathcal{F}_n^{\ell^+K^-} \right) \\ & \times \left(\prod_{k=1}^5 \prod_{l=1}^8 C_m^l(k) C_{m,K^+}^l(k) C_{u,K^+}^l(k) \right) \end{aligned}$$

where the indices i, j, m and n denote the mixed (unmixed) events, tagged by a kaon of a given charge; the index k denotes the p_K bin; and the index l denotes the signal (combinatorial background) subsample, according to the B meson charge (B^0 or B^+), and the tagging kaon category (K_T or K_R).

A total of 168 parameters are determined in the fit. To reach the convergence of the fit, we use a three-step approach. In the first step we fit only the parameters describing the B_R event fractions, whereas all the other parameters are fixed to the values obtained on simulated events. In the second step we fix the B_R fractions to the values obtained in the first step and we float only the parameters describing the resolution function. In the last step we fix the resolution parameters to the values obtained in the second step and we float again all the other parameters together with Δ_{CP} .

VII. FIT VALIDATION

Several tests are performed to validate the result. We analyze simulated events with the same procedure we use for data, first considering only the B^0 signal and adding step by step all the other samples. At each stage, the fit reproduces the generated values of Δ_{CP} (zero), and of

the other most significant parameters ($\mathcal{A}_{r\ell}$, \mathcal{A}_K , Δm , and τ_{B^0}).

We then repeat the test, randomly rejecting B^0 or \bar{B}^0 events in order to produce samples of simulated events with $\Delta_{CP} = \pm 0.005, \pm 0.01, \pm 0.025$. Also in this case the generated values are well reproduced by the fit. By removing events we also vary artificially $\mathcal{A}_{r\ell}$ or \mathcal{A}_K , testing values in the range of $\pm 10\%$. In each case, the input values are correctly determined, and an unbiased value of Δ_{CP} is always obtained. A total of 67 different simulated event samples are used to check for biases.

Pseudoexperiments are used to check the result and its statistical uncertainty. We perform 173 pseudoexperiments, each with the same number of events as the data. We obtain a value of the likelihood larger than in the data in 23% of the cases.

The distribution of the fit results for Δ_{CP} , obtained using the MIGRAD minimizer of the MINUIT [25] physics analysis tool for function minimization, is described by a Gaussian function with a central value biased by -3.6×10^{-4} (0.4σ) with respect to the nominal result. We quote this discrepancy as a systematic uncertainty related to the analysis bias.

The pull distribution is described by a Gaussian function, with a central value -0.48 ± 0.11 and rms width of 1.44 ± 0.08 . The statistical uncertainty, is, therefore, somewhat underestimated. As a cross-check, by fitting the negative log likelihood profile near the minimum with a parabola, we obtain an estimate of the statistical uncertainty from the Δ_{CP} values for which $-\log \mathcal{L} = -\log \mathcal{L}_{\min} + 0.5$ [1]. This result is in good agreement with the rms width of the distribution of the pseudoexperiments results, which we take as the statistical uncertainty of the measurement.

VIII. SYSTEMATIC UNCERTAINTIES AND CONSISTENCY CHECKS

We consider several sources of systematic uncertainty. We vary each quantity by its error, as discussed below; we repeat the measurement; and we consider the variation of the result as the corresponding systematic uncertainty. We then add in quadrature all the contributions to determine the overall systematic uncertainty.

Peaking sample composition: We vary the sample composition in the second-stage fit by the statistical uncertainties obtained in the first stage; the corresponding variation is added in quadrature to the systematic uncertainty. We then vary the fraction of B^0 to B^+ in the D^{**} peaking sample in the range $(50 \pm 25)\%$ to account for (large) violation of isospin symmetry. The fraction of the peaking contributions fixed to the simulation expectations is varied by $\pm 20\%$. Finally we conservatively vary the fraction of CP eigenstates by $\pm 50\%$.

$B\bar{B}$ combinatorial sample composition: The fraction of B^+ and B^0 in the $B\bar{B}$ combinatorial background is determined by the simulation. A difference between B^+

TABLE I. Breakdown of the main systematic uncertainties on Δ_{CP} .

Source	$\delta\Delta_{CP}(10^{-3})$
Peaking sample composition	+1.50 -1.17
Combinatorial sample composition	± 0.39
Δt resolution model	± 0.60
K_R fraction	± 0.11
$K_R \Delta t$ distribution	± 0.65
Fit bias	+0.58 -0.46
CP eigenstate description	0
Physical parameters	+0 -0.28
Total	+1.88 -1.61

and B^0 is expected when mixing takes place and the lepton is coupled to the tag side π_s from $\bar{B}^0 \rightarrow D^{*+}X$ decay. We then vary the fraction of B^0 to B^+ events in the combinatorial sample by $\pm 4.5\%$, which corresponds to the uncertainty in the inclusive branching fraction $\bar{B}^0 \rightarrow D^{*+}X$.

Δt resolution model: In order to reduce the time in the fit validation, all the parameters describing the resolution function, which show a weak correlation with $|q/p|$, are fixed to the values obtained using an iterative procedure. We perform a fit by leaving free all the parameters and we quote the difference between the two results as a systematic uncertainty.

K_R fraction: We vary the fraction of $B^+ \rightarrow K_R X$ to $B^0 \rightarrow K_R X$ by $\pm 6.8\%$, which corresponds to the uncertainty on the ratio $BR(D^{*0} \rightarrow K^- X)/BR(D^{*+} \rightarrow K^- X)$.

$K_R \Delta t$ distribution: We use half the difference between the results obtained using the two different strategies to describe the $K_R \Delta t$ distribution as a systematic uncertainty.

Fit bias: We consider two contributions: the statistical uncertainty on the validation test using the detailed simulation, and the difference between the nominal result and the central result determined from the ensemble of parametrized simulations, described in Sec. VII.

CP eigenstate description: We vary the S and C parameters describing the CP eigenstates by their statistical uncertainty as obtained from simulation.

Physical parameters: We repeat the fit, setting the value of $\Delta\Gamma$ to 0.02 ps^{-1} instead of zero. The lifetime of the B^0 and B^+ mesons and Δm are floated in the fit. Alternatively, we check the effect of fixing each parameter in turn to the world average.

By adding in quadrature all the contributions described above, and summarized in Table I, we determine an overall systematic uncertainty of $^{+1.88}_{-1.61} \times 10^{-3}$.

IX. RESULTS

We perform a blind analysis: the value of Δ_{CP} is kept masked until the study of the systematic uncertainties is completed and all the consistency checks are successfully

TABLE II. Fit results for the most significant parameters with their statistical uncertainty. Second column: Fit to the data. Third column: Fit to simulated events. Last column: Values of the parameters in the simulation at the generation stage. The detector asymmetries in the last column are obtained from the comparison of the reconstruction efficiencies for positive and negative particles in the simulation.

Parameter	Data fit	Simulation fit	From MC information
Δ_{CP}	0.0003 ± 0.0008	0.0003 ± 0.0005	0
$\mathcal{A}_{rec,e}$	0.0030 ± 0.0004	0.0097 ± 0.0002	0.0090 ± 0.0003
$\mathcal{A}_{rec,\mu}$	0.0031 ± 0.0005	0.0084 ± 0.0003	0.0091 ± 0.0003
\mathcal{A}_K	0.0137 ± 0.0003	0.0147 ± 0.0001	0.0151 ± 0.0001
τ_{B^0} (ps)	1.5535 ± 0.0019	1.5668 ± 0.0012	1.540
Δm (ps $^{-1}$)	0.5085 ± 0.0009	0.4826 ± 0.0006	0.489
$\mathcal{A}_{rec,e}$ (comb)	0.0009 ± 0.0004	0.0085 ± 0.0002	0.0095 ± 0.0002
$\mathcal{A}_{rec,\mu}$ (comb)	0.0024 ± 0.0005	0.0103 ± 0.0002	0.0102 ± 0.0002
τ_{B^0} (comb) (ps)	1.3132 ± 0.0017	1.2898 ± 0.0012	Not applicable
Δm (comb) (ps $^{-1}$)	0.4412 ± 0.0008	0.4000 ± 0.0005	Not applicable

accomplished; the values of all the other fit parameters are not masked.

After unblinding we find $\Delta_{CP} = (0.29 \pm 0.84) \times 10^{-3}$. We report in Table II the fit results for the most significant parameters. The value of Δm is consistent with the world average, while the value of τ_{B^0} is slightly larger than expected, an effect also observed in the simulation. By fixing its value to the world average, the Δ_{CP} result decreases by 0.18×10^{-3} . This effect is taken into account in the systematic uncertainty computation. Figures 4 and 5 show the fit projections for Δt and $\cos \theta_{\ell K}$, respectively.

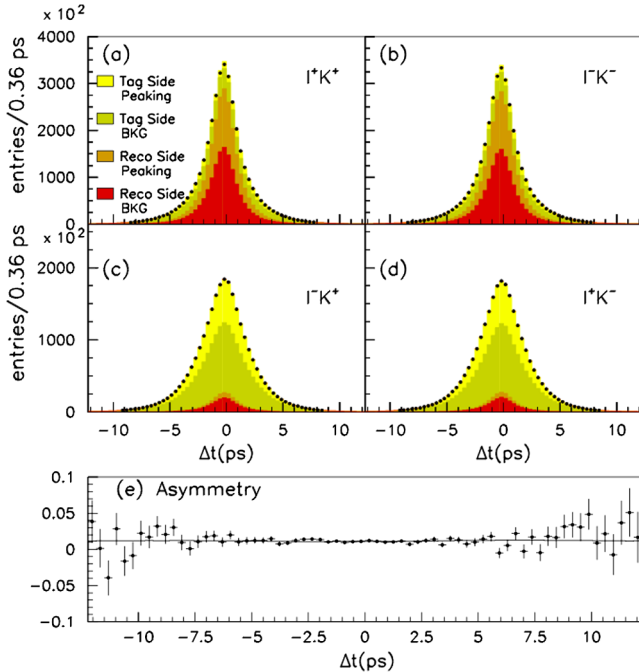


FIG. 4. Distribution of Δt for the continuum-subtracted data (points with error bars) and fitted contributions from peaking K_T , background K_T , peaking K_R and background K_R , for (a) ℓ^+K^+ events, (b) ℓ^-K^- events, (c) ℓ^-K^+ events, (d) ℓ^+K^- events, (e) raw asymmetry between ℓ^+K^+ and ℓ^-K^- events.

A sizable charge asymmetry is observed at the reconstruction stage, for both e and μ reconstruction and at the K tagging stage, somewhat smaller than that observed in the simulation. As the size of \mathcal{A}_{ℓ} is the same for the e and the μ samples, it is reasonable to suppose that the main source of charge asymmetry at the B^0 reconstruction stage is due to the π_s .

Recently the BABAR collaboration published a measurement of the asymmetry \mathcal{A}_{CP} between same-sign inclusive dilepton samples $\ell^+\ell^+$ and $\ell^-\ell^-$ using the complete recorded data set [8]. The systematic errors of the two analyses are essentially uncorrelated. The correlation of the statistical errors is estimated to be on a level below 10%.

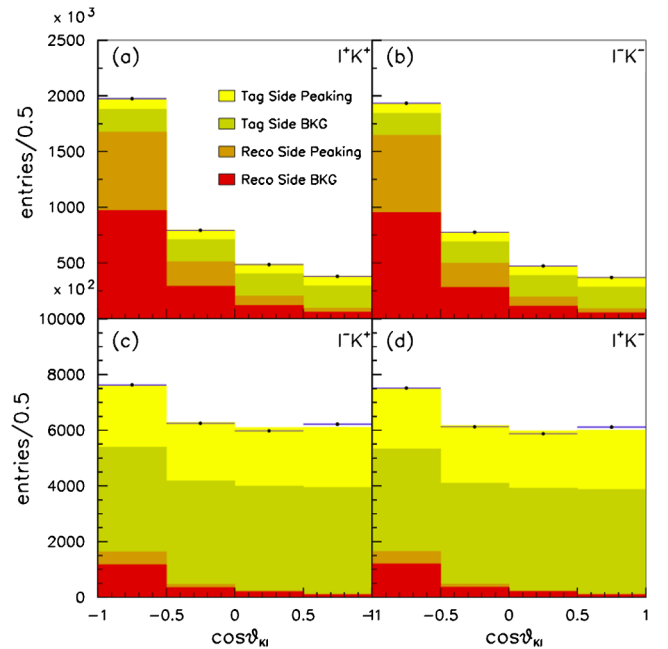


FIG. 5. Distribution of $\cos \theta_{\ell K}$ for the continuum-subtracted data (points with error bars) and fitted contributions from peaking K_T , background K_T , peaking K_R and background K_R , for (a) ℓ^+K^+ events, (b) ℓ^-K^- events, (c) ℓ^-K^+ events, (d) ℓ^+K^- events.

X. CONCLUSIONS

We present a new precise measurement of the parameter governing CP violation in $B^0\text{-}\bar{B}^0$ oscillations. With a technique based on partial $\bar{B}^0 \rightarrow D^{*+}\ell^-\bar{\nu}_\ell$ reconstruction and K tagging we find

$$\Delta_{CP} = 1 - |q/p| = (0.29 \pm 0.84^{+1.88}_{-1.61}) \times 10^{-3},$$

where the first uncertainty is statistical and the second is systematic. The corresponding asymmetry,

$$\mathcal{A}_{CP} \simeq 2 \left(1 - \left| \frac{q}{p} \right| \right) = (0.06 \pm 0.17^{+0.38}_{-0.32})\%,$$

is consistent with and competitive with the results from dilepton measurements at the B factories, LHCb [13] and $D0$ [9]. We observe no deviation from the SM expectation [2].

ACKNOWLEDGMENTS

We are grateful for the extraordinary contributions of our PEP-II colleagues in achieving the excellent luminosity and

machine conditions that have made this work possible. The success of this project also relies critically on the expertise and dedication of the computing organizations that support *BABAR*. The collaborating institutions wish to thank SLAC for its support and the kind hospitality extended to them. This work is supported by the U.S. Department of Energy and National Science Foundation, the Natural Sciences and Engineering Research Council (Canada), the Commissariat à l’Energie Atomique and Institut National de Physique Nucléaire et de Physique des Particules (France), the Bundesministerium für Bildung und Forschung and Deutsche Forschungsgemeinschaft (Germany), the Istituto Nazionale di Fisica Nucleare (Italy), the Foundation for Fundamental Research on Matter (The Netherlands), the Research Council of Norway, the Ministry of Education and Science of the Russian Federation, Ministerio de Economía y Competitividad (Spain), the Science and Technology Facilities Council (United Kingdom) and the Binational Science Foundation (U.S.-Israel). Individuals have received support from the Marie-Curie IEF program (European Union) and the A. P. Sloan Foundation (USA).

-
- [1] K. A. Olive *et al.* (Particle Data Group), *Chin. Phys. C* **38**, 090001 (2014).
 - [2] A. Lenz and U. Nierste, *J. High Energy Phys.* **06** (2007) 072.
 - [3] A. Lenz, U. Nierste, J. Charles, S. Descotes-Genon, H. Lacker, S. Monteil, V. Niess, and S. T’Jampens, *Phys. Rev. D* **86**, 033008 (2012); J. Charles *et al.*, *Phys. Rev. D* **84**, 033005 (2011).
 - [4] J. P. Lees *et al.* (*BABAR* Collaboration), *Phys. Rev. Lett.* **111**, 101802 (2013).
 - [5] D. E. Jaffe *et al.* (CLEO Collaboration), *Phys. Rev. Lett.* **86**, 5000 (2001).
 - [6] E. Nakano *et al.* (Belle Collaboration), *Phys. Rev. D* **73**, 112002 (2006).
 - [7] B. Aubert *et al.* (*BABAR* Collaboration), *Phys. Rev. Lett.* **96**, 251802 (2006).
 - [8] J. P. Lees *et al.* (*BABAR* Collaboration), *Phys. Rev. Lett.* **114**, 081801 (2015).
 - [9] V. M. Abazov *et al.* ($D0$ Collaboration), *Phys. Rev. D* **89**, 012002 (2014).
 - [10] V. M. Abazov *et al.* ($D0$ Collaboration), *Phys. Rev. Lett.* **110**, 011801 (2013).
 - [11] R. Aaij *et al.* (LHCb Collaboration), *Phys. Lett. B* **728**, 607 (2014).
 - [12] V. M. Abazov *et al.* ($D0$ Collaboration), *Phys. Rev. D* **86**, 072009 (2012).
 - [13] R. Aaij *et al.* (LHCb Collaboration), *Phys. Rev. Lett.* **114**, 041601 (2015).
 - [14] G. Borissov and B. Hoeneisen, *Phys. Rev. D* **87**, 074020 (2013).
 - [15] B. Aubert *et al.* (*BABAR* Collaboration), *Nucl. Instrum. Methods Phys. Res., Sect. A* **479**, 1 (2002).
 - [16] B. Aubert *et al.* (*BABAR* Collaboration), *Nucl. Instrum. Methods Phys. Res., Sect. A* **729**, 615 (2013).
 - [17] J. P. Lees *et al.* (*BABAR* Collaboration), *Nucl. Instrum. Methods Phys. Res., Sect. A* **726**, 203 (2013).
 - [18] D. Lange, *Nucl. Instrum. Methods Phys. Res., Sect. A* **462**, 152 (2001).
 - [19] S. Agostinelli *et al.* (GEANT4), *Nucl. Instrum. Methods Phys. Res., Sect. A* **506**, 250 (2003).
 - [20] G. C. Fox and S. Wolfram, *Phys. Rev. Lett.* **41**, 1581 (1978).
 - [21] E. Barberio, B. van Eijk, and Z. Was, *Comput. Phys. Commun.* **66**, 115 (1991); E. Barberio and Z. Was, *Comput. Phys. Commun.* **79**, 291 (1994).
 - [22] D. Boutigny *et al.*, SLAC Report No. SLAC-R-504, 1998.
 - [23] O. Long, M. Baak, R. N. Cahn, and D. Kirkby, *Phys. Rev. D* **68**, 034010 (2003).
 - [24] A. A. Logunov, L. D. Soloviev, and A. N. Tavkhelidze, *Phys. Lett.* **24B**, 181 (1967); K. G. Chetyrkin and N. V. Krasnikov, *Nucl. Phys.* **B119**, 174 (1977); K. G. Chetyrkin, N. V. Krasnikov, and A. N. Tavkhelidze, *Phys. Lett.* **76B**, 83 (1978).
 - [25] F. James and M. Roos, *Comput. Phys. Commun.* **10**, 343 (1975).